

Gamma-Ray Decay of the Low-Lying Levels of Cl^{34}

K. A. Snover, J. M. McDonald, and D. B. Fossan

State University of New York, Stony Brook, New York 11790

and

E. K. Warburton

Brookhaven National Laboratory, Upton, New York 11973

(Received 5 April 1971)

The excitation energies and γ -ray decay modes of the low-lying states of Cl^{34} have been studied using the $\text{S}^{32}(\text{He}^3, p\gamma)\text{Cl}^{34}$ reaction. Some lifetime limits were obtained by the Doppler-shift-attenuation method. The lifetimes of the $(J^\pi, T) = (1^+, 0)$ levels at 461 and 666 keV, and the $(2^+, 0)$ level at 1230 keV were measured to be 7.1 ± 0.7 , 12.8 ± 1.0 , and 19.4 ± 1.4 psec, respectively, using the recoil-distance (plunger) technique with the $\text{P}^{31}(\alpha, n\gamma)\text{Cl}^{34}$ reaction. The transition strengths from these three levels are discussed qualitatively in terms of calculations involving simple configurations, and are compared with recent detailed shell-model calculations.

I. INTRODUCTION

Cl^{34} is an odd-odd self-conjugate nucleus and, like others of this class, is a rich source of nuclear-structure information and a fruitful testing ground for nuclear models. Very recently, there has been a great deal of experimental work on this nucleus. The first comprehensive study of the γ -ray decay modes was the $\text{S}^{33}(p, \gamma)\text{Cl}^{34}$ work of Gräber and Harris.¹ The $\text{S}^{32}(\text{He}^3, p\gamma)\text{Cl}^{34}$ and $\text{P}^{31}(\alpha, n\gamma)\text{Cl}^{34}$ results of Brandolini and co-workers,^{2,3} of Sykes,⁴ and of Deluca, Lawson, and Chagnon⁵ soon followed. Before these studies only the ground state and first excited state had definite spin-parity assignments.⁶ Now, as a result of these γ -ray decay studies¹⁻⁵ and several direct-reaction studies,^{7,8} there are definite spin-parity assignments for the first six states of Cl^{34} .

The presently available information on the excitation energies, γ -ray decay modes, and spin-parity assignments of the first seven states of Cl^{34} is summarized in Fig. 1. Some results from the present work are included in this figure.

The present work consists of two parts. In the first, the $\text{S}^{32}(\text{He}^3, p\gamma)\text{Cl}^{34}$ reaction was used to study the energies and decay modes of the γ rays emitted by the low-lying levels of Cl^{34} . Some information on the lifetimes of the states was also obtained from the observation of Doppler shifts. This work is reported in Sec. II. In Sec. III results for the mean lives of the 461-, 666-, and 1230-keV states of Cl^{34} are reported. The $\text{P}^{31}(\alpha, n\gamma)\text{Cl}^{34}$ reaction was used to populate the states, and the recoil-distance method⁹⁻¹¹ was used to determine the mean lives. Section IV contains a discussion of the lifetime measurements.

II. EXCITATION ENERGIES AND DECAY MODES

$\text{Ge}(\text{Li})$ spectra of γ rays emitted following the bombardment of a natural sulfur (95.0% S^{32} , 4.2% S^{34}) target with a 6.8-MeV He^3 beam were recorded and analyzed to obtain the excitation energies and branching ratios reported herein. A doubly ionized He^3 beam of ~ 10 nA was provided by the Brookhaven National Laboratory 3.5-MeV Van de Graaff accelerator. γ rays were detected by a 40-cc coaxial $\text{Ge}(\text{Li})$ detector placed 8 cm from the sulfur target and at either 90 or 0° to the beam axis. The spectra were recorded using a 4096-channel analog-to-digital converter (ADC).

Energies of the first four levels of Cl^{34} were measured first in a high-dispersion study of the low-energy (<862 keV) γ rays. The mixed-source technique was used, and the detection angle was 90°. One spectrum was recorded with sources of Mn^{54} , Cs^{137} , and Ir^{192} placed so that the intensities of the γ rays from these sources were comparable with the intensities of the $\text{S}^{32} + \text{He}^3$ γ rays. A second spectrum was taken using sources of Mn^{54} , Cs^{137} , Ir^{192} , Bi^{207} , and Th^{228} . Portions of this spectrum are shown in Fig. 2. A third spectrum, taken to obtain the energy of the first excited state at 146 keV in Cl^{34} , was recorded with the beam off after buildup of the 32-min⁶ activity due to this metastable state. Sources of Co^{57} and Ir^{192} were used in this measurement. The energies of the γ rays emitted by Mn^{54} , Cs^{137} , Ir^{192} , Bi^{207} , and Th^{228} were taken from the compilation of Marion¹²; the Co^{57} energies and some of the Ir^{192} energies were from the work of Greenwood, Helmer, and Gehrke.¹³

For all three spectra the method of analysis

was the same. First, the positions of the full-energy peaks were determined as follows. A least-squares fit of an exponential was made to the data points in the wings of a γ -ray full-energy peak (or peaks). Subsequently, a least-squares fit was made to the peak assuming a Gaussian superimposed on the predetermined exponential background. The results of six such fits are illustrated in Fig. 2. The Gaussian fits were restricted to the channels for which the peak intensity was $\geq 25\%$ of the peak intensity. Tests were made to determine the sensitivity of the peak position to the assumed background level and to the region of channels used in the Gaussian fitting. The peak positions were quite insensitive to reasonable changes in both. The uncertainties in the γ -ray energies in Table I include an estimate of this systematic error.

The second step was to fit the polynomial

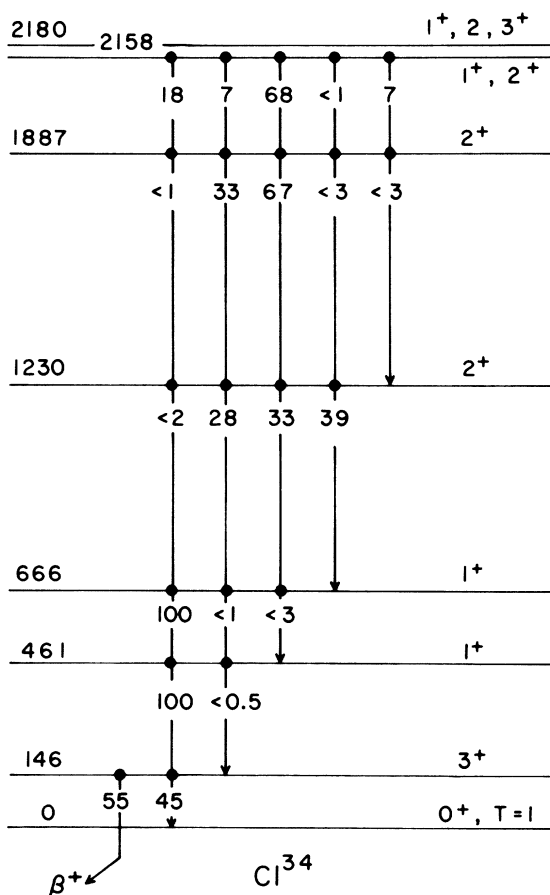


FIG. 1. Energy-level scheme of Cl^{34} . The excitation energies (in keV) are from the present work, the γ -ray branching ratios are from this and previous work (see Table III), and the spin-parity assignments are from Refs. 1-7.

$$E_{\gamma} = \sum_{n=0}^m a_n x^n \quad (1)$$

to the radioactive peaks of known energy. The uncertainties in the peak positions x were taken account of in the least-squares analysis, as well as the uncertainties associated with the E_{γ} . As an example of the results of this procedure, consider the spectrum recorded with Mn^{54} , Cs^{137} , Ir^{192} , Bi^{207} , and Th^{228} sources. 16 γ -ray peaks with energies ranging from 238 to 834 keV were included in the least-squares fit to Eq. (1). χ^2 , the measure of the goodness of fit, varied with the polynomial degree, m , of Eq. (1) as follows:

m	2	3	4	5
χ^2	34.5	4.7	0.8	0.8

χ^2 has been normalized by dividing by the degrees of freedom and so its expectation value is unity. The data, then, are well described by a polynomial of degree 4, and this comparison gives conclusive evidence for monotonically varying nonlinearities in the detector-amplifier-analyzer system, such as have been discussed recently by Greenwood, Helmer, and Gehrke.¹³ Similar results were obtained for the other two spectra. The energies of Table I, which are the weighed averages of the two results, were taken from the calibration curves with $m = 4$. It can be seen in Fig. 2 that the radioactive lines were chosen to form close-lying doublets with the lines of interest. This insured that any uncertainties due to local nonlinearities were minimized. The excitation energies of the first four excited states of Cl^{34} listed in Table II result from the γ -ray energies of Table I.

The energies of the next three levels were obtained from a 90° spectrum taken with a dispersion of 0.992 keV/channel and including γ rays with energies up to 4082 keV. For this spectrum the energy calibration was internal and was based mainly on the γ rays of Table I and the S^{34} 2127- and 3304-keV γ rays⁶ from the β decay of Cl^{34*} . As can be seen from Table III, two γ rays were

TABLE I. Low-energy γ rays from $\text{S}^{32,34} + \text{He}^3$.

E_{γ} (keV)	Level assignment	Reaction
146.36 ± 0.03	$\text{Cl}^{34}(1 \rightarrow 0)$	$\text{S}^{32}(\text{He}^3, p)\text{Cl}^{34}$
461.00 ± 0.04	$\text{Cl}^{34}(2 \rightarrow 0)$	$\text{S}^{32}(\text{He}^3, p)\text{Cl}^{34}$
564.68 ± 0.06	$\text{Cl}^{34}(4 \rightarrow 3)$	$\text{S}^{32}(\text{He}^3, p)\text{Cl}^{34}$
665.56 ± 0.05	$\text{Cl}^{34}(3 \rightarrow 0)$	$\text{S}^{32}(\text{He}^3, p)\text{Cl}^{34}$
769.25 ± 0.07	$\text{Cl}^{34}(4 \rightarrow 2)$	$\text{S}^{32}(\text{He}^3, p)\text{Cl}^{34}$
788.46 ± 0.20	$\text{Cl}^{36}(1 \rightarrow 0)$	$\text{S}^{34}(\text{He}^3, p)\text{Cl}^{36}$
810.51 ± 0.16	$\text{Cl}^{33}(1 \rightarrow 0)$	$\text{S}^{32}(\text{He}^3, d)\text{Cl}^{33}$
840.91 ± 0.05	$\text{S}^{33}(1 \rightarrow 0)$	$\text{S}^{32}(\text{He}^3, 2p)\text{S}^{33}$ $+\text{S}^{34}(\text{He}^3, \alpha)\text{S}^{33}$

observed which were assigned to the decay of the fifth excited state and four γ -ray peaks were assigned to the decay of the sixth excited state. In addition, two γ -ray peaks had the right energy to be assigned to the 2.18–0.15 and 2.18–0.46-MeV transitions, and the excitation energy for the seventh excited state, resulting from our determination of these two γ -ray energies, is given in Table II. It should be remarked that our identification of the γ -ray peaks is based mainly on their energies and, therefore, relies heavily on previous coincidence studies.²⁻⁴

For both the low- and high-dispersion gains, spectra were taken at 0° as well as 90° . From these spectra information was obtained on γ -ray Doppler shifts. From the 0.209-keV/channel spectra it was determined that the Cl^{34} γ rays of Table I all had 0 – 90° Doppler shifts of <0.1 keV. For comparison, the expected shift is 0.51% of E_γ for an average He^3 energy of 5.0 MeV and a $\text{S}^{32}(\text{He}^3, p)\text{-Cl}^{34}$ angular distribution symmetric in the center-of-mass system. These results are consistent with previous results² which indicate that the 0.46-, 0.67-, and 1.23-MeV levels all have mean lives long compared to the stopping time of Cl^{34} ions in solids. The γ rays emitted by the next three levels all had observable Doppler shifts. Those emitted by the 1887- and 2180-keV levels had shifts significantly less than the kinematical shift, thus indicating lifetimes for the initial states comparable (within, say, a factor of 3) to the slowing down time of ~ 0.5 psec. The γ rays emitted by the 2158-MeV level appeared to have the full kinematical shifts; i.e., $\tau \ll 0.5$ psec.

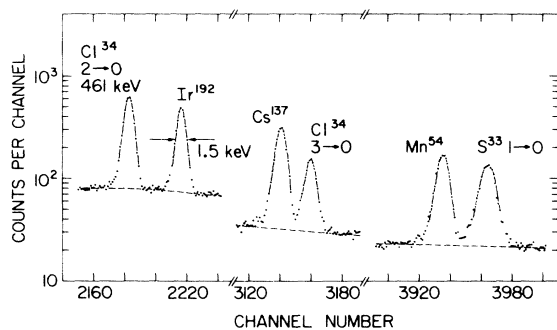


FIG. 2. Portions of a 40-cc Ge(Li) γ -ray spectrum taken at 90° to the 6.8-MeV He^3 beam and 8 cm from the natural sulfur target using a 4096-channel ADC. The dispersion is 0.209 keV/channel. The dashed lines indicate the exponential backgrounds assumed in the Gaussian fits to the six indicated full-energy peaks. The solid lines through the data points indicate the regions included in the Gaussian least-squares fits. The energies of the radioactive γ rays were taken from Ref. 11 as follows: Ir^{192} , 468.053 ± 0.014 keV; Cs^{137} , 661.635 ± 0.076 keV; Mn^{54} , 834.81 ± 0.03 keV.

These results are also consistent with previous, more quantitative results.³

Branching-ratio information was extracted from the various Ge(Li) spectra. The effects of any anisotropies were approximately taken account of by forming the sum of the 90 and 0° spectra normalized in the ratio 2:1. This accounts for terms in $P_2(\cos\theta_\gamma)$. The anisotropies were small and $P_4(\cos\theta_\gamma)$ terms were considered to have negligible effect. The branching ratios obtained in this work are compared with previous results in Table III. We adopt the "subjectively weighted" results given in the last column of Table III.

III. LIFETIME MEASUREMENTS OF THE 461-, 666-, AND 1230-keV LEVELS OF Cl^{34}

A. Neutron- γ Coincidence Measurements

The $\text{P}^{31}(\alpha, n\gamma)\text{Cl}^{34}$ reaction was explored at various α -particle bombarding energies between 8 and 11 MeV, using a 1-mg/cm² Zn_3P_2 target evaporated onto a thick Ta backing. The neutrons were detected in a NE213 liquid scintillator positioned near $+30^\circ$ with respect to the incident beam, and the γ rays were detected in a Ge(Li) detector placed at -90° . Pulse-shape discrimination was employed to separate the neutron pulses from the γ -ray pulses in the neutron detector.¹⁴ A γ -ray spectrum in coincidence with neutrons obtained at $E_\alpha = 11.0$ MeV is shown in the bottom half of Fig. 3, and a singles γ -ray spectrum obtained at the same energy is shown in the top half of Fig. 3. The 461- and 666-keV γ rays from Cl^{34} are clearly seen in both the singles spectrum and the coincidence spectrum, and the γ rays from the 1230–461 and 1230–666 transitions (where the energies are in keV) are also evident. The other coincident γ rays labeled in the lower half of Fig. 3 correspond to known γ -ray transitions in Cl^{34} (see Table III). The unidentified lines in the singles spec-

TABLE II. Excitation energies of the low-lying levels of Cl^{34} .

Level	Present work (keV)	Previous work ^a (keV)
1	146.36 ± 0.03	146.2 ± 0.3 ^b
2	461.00 ± 0.04	461.5 ± 0.3
3	665.55 ± 0.05	664.6 ± 0.3
4	1230.24 ± 0.07	1228.8 ± 0.7
5	1887.1 ± 1.6	1885.9 ± 1.6
6	2158.0 ± 0.5	2158.4 ± 1.2
7	2180.1 ± 1.5	2179.4 ± 1.4 ^c

^a Except for the first and last levels these are from Ref. 1.

^b Reference 5.

^c Reference 3.

TABLE III. Branching ratios for the low-lying levels of Cl^{34} .

Level	E_i (keV)	E_f (keV)	E_γ (keV)	Present results	Branching ratio		Adopted values
					Refs. 2, 3	Ref. 1	
2	461.00	0	461.00	100	100	100	100
		146.36	314.64	<0.5	<3	<5	<0.5
3	665.55	0	665.55	100	100	100	100
		146.36	519.19	<1	<3	<5	<1
		461.00	204.55	<3	<3	<5	<3
4	1230.24	0	1230.24	<4	<2	<2	<2
		146.36	1083.88	27.5 ± 2	32 ± 6	23 ± 7	28 ± 2
		461.00	769.24	31.8 ± 2	37 ± 5	29 ± 5	33 ± 2
		665.55	564.69	40.7 ± 2	31 ± 4	48 ± 10	39 ± 2
5	1887.10	0	1887.10	<14	<1	<8	<1
		146.36	1740.74	32.8 ± 2	39 ± 4	50 ± 20	33 ± 2
		461.00	1426.10	67.2 ± 2	61 ± 4	50 ± 18	67 ± 2
		665.55	1221.55	...	<3	<8	<3
		1230.24	656.86	<8	<3	...	<3
6	2158.0	0	2158.00	17.1 ± 2	27 ± 8	24 ± 9	18 ± 2
		146.36	2011.64	7.1 ± 2	<8	<6	7 ± 2
		461.00	1697.00	68.8 ± 3	73 ± 8	64 ± 11	68 ± 3
		665.55	1492.45	<1	10	<2	<1
		1230.24	927.76	7.0 ± 2	...	12 ± 4	7 ± 2
		1887.10	270.90	<1	<1

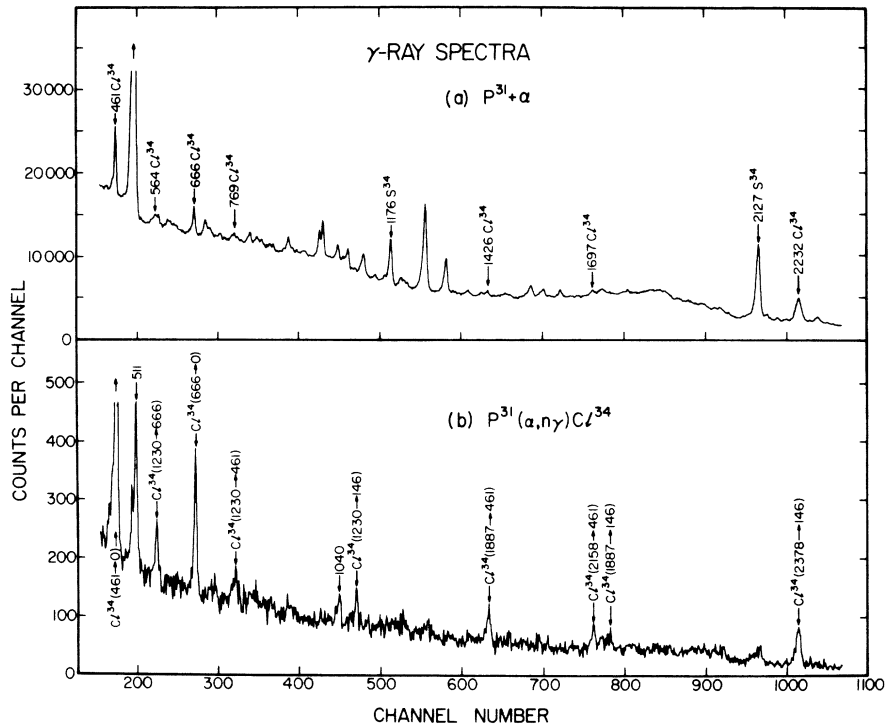


FIG. 3. γ spectra from the α -particle bombardment of a Zn_3P_2 target at $E_\alpha = 11.0$ MeV. The upper spectrum (a) is a singles γ -ray spectrum and the lower spectrum (b) is an α - γ coincidence spectrum obtained using a Ge(Li) detector for the γ rays, and an NE213 liquid scintillator for the neutrons. Transitions labeled Cl^{34} are from the $\text{P}^{31}(\alpha, n\gamma)\text{Cl}^{34}$ reaction, and transitions labeled S^{34} are from the reaction $\text{P}^{31}(\alpha, p\gamma)\text{S}^{34}$.

trum may arise from other reactions on P^{31} and from reactions on the zinc in the target.

B. Lifetime Measurements

The lifetimes of the $(J^\pi, T) = (1^+, 0)$ levels in Cl^{34} at excitation energies of 461 and 666 keV, and the $(2^+, 0)$ level at 1230 keV were measured using the recoil-distance (plunger) technique.⁹⁻¹¹ The plunger apparatus used in these measurements has been described previously.¹⁰ The excited Cl^{34} nuclei were produced in the $P^{31}(\alpha, n)Cl^{34}$ reaction using an α -particle beam from the Stony Brook tandem Van de Graaff accelerator. Lifetime measurements were made at $E_\alpha = 8.3$ MeV for the 461- and 666-keV states, and at $E_\alpha = 9.3$ MeV for the 1230-keV state. The target consisted of approximately $100 \mu g/cm^2$ of Zn_3P_2 evaporated onto a $4\text{-mg}/cm^2$ gold foil. The target was positioned in the plunger apparatus by means of a V-groove, O-ring arrangement designed to hold the target surface flat. The target was oriented so that the beam would pass through the gold backing before striking the target material. Because of the endothermic nature of the $P^{31}(\alpha, n)Cl^{34}$ reaction, the recoiling Cl^{34} nuclei in the excited states of interest were kinematically constrained to travel inside a forward cone of 9° half angle. The recoils were stopped in a flat gold "plunger" which could be positioned at variable distances D from the target. The γ rays produced by the decay of the recoiling nuclei were detected with a 15-cc Ge(Li)

detector positioned at 0° with respect to the beam direction.

The γ rays produced by the recoiling Cl^{34} nuclei which decay in flight exhibit a Doppler-shifted energy at 0° given by

$$E_s = E_0(1 + v/c),$$

where v is the component of the recoil velocity in the beam direction. The γ rays emitted from the excited Cl^{34} nuclei that have stopped in the plunger material have an unshifted energy E_0 and thus may be distinguished from the shifted γ rays. The intensities of the unshifted peak I_0 and the Doppler-shifted peak I_s are given by^{9, 10}

$$I_0 = Ne^{-D/v\tau}$$

and

$$I_s = N(1 - e^{-D/v\tau}),$$

where N is the total intensity of γ rays ($N = I_0 + I_s$), and τ is the mean lifetime of the initial state. The ratio $R = I_0/(I_0 + I_s)$ is given by

$$R = e^{-D/v\tau},$$

and hence a measurement of R as a function of D provides the mean lifetime τ with a knowledge of v . In practice, one must make corrections to these simple relations for a number of effects¹⁰ which have not been discussed, such as the presence of a finite distribution of recoil velocities. These corrections, which are all small in the present case, will be mentioned briefly toward the end of this section.

In the plunger measurements, the 461-0, 666-0, 1230-461, and 1230-666 transitions in

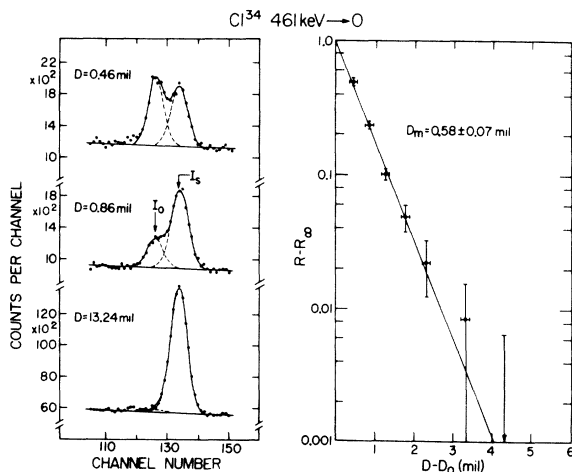


FIG. 4. γ -ray spectra and lifetime curve for the 461-keV $\rightarrow 0$ transition. The left portion of the figure displays the γ -ray spectra in the region of the 461 $\rightarrow 0$ transition, measured at three different plunger displacements D . The right portion of the figure is a logarithmic lifetime plot of $R - R_\infty$ vs $D - D_0$, with $R_\infty = 0.018 \pm 0.005$. The curves through the data points represent least-squares fits to the data as described in the text.

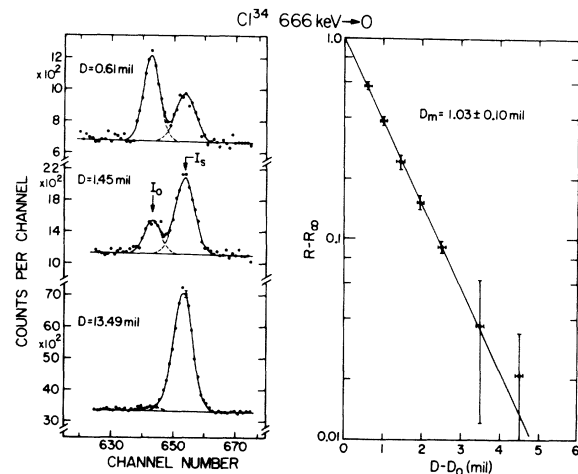


FIG. 5. γ -ray spectra and lifetime curves for the 666-keV $\rightarrow 0$ transition. The figure details are similar to the description given in the caption of Fig. 4, with $R_\infty = 0.028 \pm 0.007$.

TABLE IV. Lifetime analysis.

Transition (keV)	D_m (mil) ^a	v/c (%)	Uncorrected τ (psec) ^b	Final τ (psec) ^c
461 \rightarrow 0	0.58 ± 0.07	0.647 ± 0.008	7.61 ± 0.92	7.1 ± 0.7
	0.48 ± 0.08	0.612 ± 0.007	6.61 ± 1.10	
666 \rightarrow 0	1.04 ± 0.10	0.639 ± 0.008	13.66 ± 1.37	12.8 ± 1.0
	0.90 ± 0.11	0.606 ± 0.005	12.57 ± 1.54	
1230 \rightarrow 461	1.55 ± 0.15	0.647 ± 0.015	20.34 ± 1.97	19.4 ± 1.4
1230 \rightarrow 666	1.42 ± 0.14	0.645 ± 0.011	18.64 ± 1.844	

^aIn units of 10^{-3} inches.

^bComputed from the relation $\tau = D_m/v$, in units of 10^{-12} sec.

^cIncluding geometry, solid-angle, counter-efficiency, and velocity-distribution corrections (see text).

Cl^{34} were studied. The 461 \rightarrow 0 and 666 \rightarrow 0 transitions were studied simultaneously at $E_\alpha = 8.3$ MeV, and the 1230 \rightarrow 461 and 1230 \rightarrow 666 transitions were studied together at $E_\alpha = 9.3$ MeV. The spectra were recorded in a 1024-channel pulse-height analyzer with an appropriate bias to obtain a dispersion of 0.4 keV per channel. The energy resolution was about 2.4 keV full width at half maximum for these γ rays. The spectra were analyzed in a computerized least-squares fitting procedure. In the first step the background in the region of the I_0 and I_s peaks was fit with a linear function. In the second step the I_0 and I_s intensities were determined by simultaneously fitting two analytic peak shapes to the data with predetermined background. The peak shape used to fit the I_0 intensity was Gaussian, while the I_s shape included an asymmetry parameter in addition to the usual Gaussian form. The left-hand portions of Figs. 4 through 7

illustrate typical spectra of interest, and the fits obtained by this analysis. The intensities I_0 and I_s extracted in this fashion were used to compute the ratios R , as a function of D .

The measured ratio R as a function of D was then fit with an expression of the form

$$R = e^{-(D-D_0)/D_m} + R_\infty,$$

where D_0 , D_m , and R_∞ were treated as parameters. D_0 represents the zero of the plunger displacement and D_m is related to the mean lifetime by $D_m = v\tau$. A nonzero value of R_∞ might be obtained, for example, if the plunger surface had been contaminated by target material or if some of the recoils stopped in the material due to large-angle scattering.

The measured and calculated values of R as a function of D are displayed in the right-hand portions of Figs. 4–7. These figures display $R - R_\infty$.

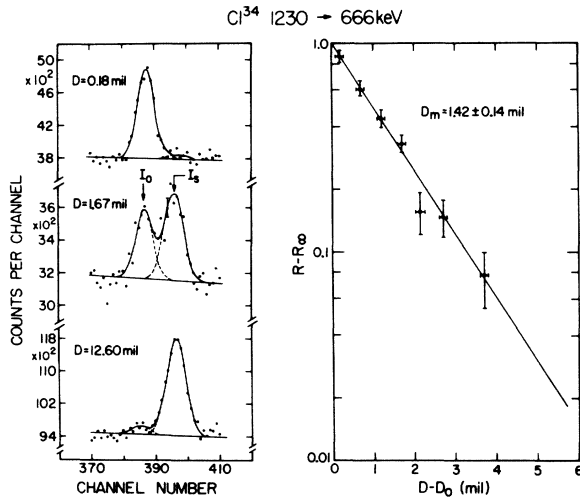


FIG. 6. γ -ray spectra and lifetime curves for the 1230 \rightarrow 666-keV transition. The figure details are similar to the description given in the caption of Fig. 4, with $R_\infty = 0.070 \pm 0.015$.

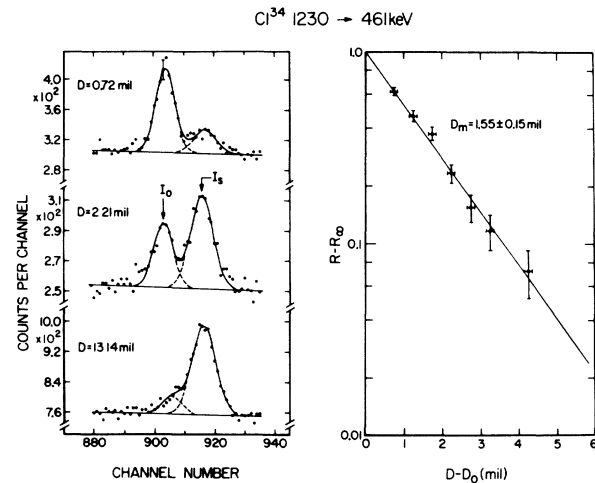


FIG. 7. γ -ray spectra and lifetime curves for the 1230 \rightarrow 461-keV transition. The figure details are similar to the description given in the caption of Fig. 4, with $R_\infty = 0.139 \pm 0.015$.

versus $D - D_0$, where the additive constants R_∞ and D_0 were determined by the fitting process. The values of R_∞ were determined primarily by measurements at large $D - D_0$ (≈ 13 mil) which are not shown in the figures. For the 461 \rightarrow 0 and 666 \rightarrow 0 transitions, a second series of data points were obtained which were similar to the data displayed in Figs. 4 and 5. All of these data were used to arrive at the results given in Table IV. The average projection v of the recoil velocity in the direction of the incident beam was determined for each transition from the separation of the centroids of I_s and I_0 . Column 4 of Table IV contains the mean lifetime values computed from the relation $\tau = D_m/v$. A number of small corrections were then applied to these results, the most important being the recoil-velocity distribution correction,¹⁰ which was computed from the γ -ray spectra to be between 1 and 3% for the various transitions. The geometry, solid-angle, and counter-efficiency corrections described in Ref. 10 yielded a total correction of 0.6% for these measurements. The final lifetime values are listed in the last column of Table IV. These results for the lifetimes of the 461- and 666-keV levels replace the preliminary values, quoted previously,¹⁵ which contained a systematic error due to partial feeding from the 1230-keV level.

IV. DISCUSSION OF THE LIFETIME MEASUREMENTS

The mean lifetimes of the 461-, 666-, and 1230-keV levels of Cl^{34} deduced from this work are shown in Table V along with the lifetime values measured in previous work² by the Doppler-shift

TABLE V. Lifetimes of the 461-, 666-, and 1230-keV levels of Cl^{34} .

Level	E_{ex} (keV)	Mean lifetime (psec)	
		Present work	Previous work Ref. 2
2	461.00	7.1 ± 0.7	9 ± 4
3	665.55	12.8 ± 1.0	14^{+11}_{-6}
4	1230.24	19.4 ± 1.4	> 14

attenuation method (DSAM). The present work is in good agreement with the less accurate DSAM measurements. The experimental $M1$ and $E2$ transition strengths obtained from the present lifetime results are listed in Table VI in units of the Weisskopf single-particle estimates.¹⁶ The $M1$ strengths were computed using the present lifetime and branching-ratio measurements along with the $E2/M1$ mixing ratios quoted previously^{2,3} for transitions from the 1230-keV level. The $M1$ $\Delta T = 0$ transition strengths from the $(2^+, 0)$ level are all weak, which is consistent with Morpurgo's rule.¹⁷ The $M1$ $\Delta T = 1$ transitions 461 \rightarrow 0 and 666 \rightarrow 0 are also slow compared with the Weisskopf single-particle estimate.

The slowness of the $M1$ $\Delta T = 1$ transitions may be understood on the basis of the dominant shell-model configuration involved. The results of recent single-nucleon-transfer reactions^{7,8} into Cl^{34} suggest the dominant configurations $[s_{1/2}^3 d_{3/2}^3]_{1^+,0}$ and $[s_{1/2}^4 d_{3/2}^2]_{1^+,0}$ for the 461- and 666-keV levels, respectively, based on a Si^{28} core which closes the $d_{5/2}$ subshell. In this approximation the ground state should be predominantly $[s_{1/2}^4 d_{3/2}^2]_{0^+,1}$. The $s^3 d^3 - s^4 d^2$ transition is forbidden, since the $M1$

TABLE VI. A comparison of the experimental $B(M1)$ and $B(E2)$ reduced transition strengths in Cl^{34} , deduced from the present lifetime and branching ratio measurements, expressed in units of Weisskopf estimate B_w . [See Ref. 16. For completeness, we note: $B(M1)_w = 1.79 \mu_N^2$ and for $A = 34$, $B(E2)_w = 6.54 e^2 F^4$.]

Transition (keV)	$(J^\pi, T)_i$	$(J^\pi, T)_f$	$[B(M1) \times 10^2]/B(M1)_w$	$B(E2)/B(E2)_w$	$x(E2/M1)^a$
461 \rightarrow 0	$(1^+, 0)$	$(0^+, 1)$	4.5 ± 0.4		
461 \rightarrow 147		$(3^+, 0)$		< 27	
666 \rightarrow 0	$(1^+, 0)$	$(0^+, 1)$	0.83 ± 0.06		
666 \rightarrow 147		$(3^+, 0)$		< 2.5	
1230 \rightarrow 0	$(2^+, 0)$	$(0^+, 1)$		< 0.1	
1230 \rightarrow 147		$(3^+, 0)$	$0.006^{+0.024}_{-0.004}$	$1.0^{+0.1}_{-0.8}$	2.2 ± 1.8
1230 \rightarrow 461		$(1^+, 0)$	$0.05^{+0.03}_{-0.02}$	$4.4^{+1.0}_{-2.2}$	1.2 ± 0.5
1230 \rightarrow 666		$(1^+, 0)$	0.32 ± 0.03	5.4 ± 2.7	0.37 ± 0.09

^aReferences 2 and 3. Note also that the uncertainties in the reduced strengths for the mixed transitions arise predominantly from the large uncertainties in the mixing ratios and are thus directly correlated. For example, if the 1230 \rightarrow 461 transition has a $B(M1)$ of 0.08×10^{-2} W.u., then the $B(E2)$ must be 2.2 W.u.

operator cannot change l . The $[d_{3/2}^2]_{1^+,0} \rightarrow [d_{3/2}^2]_{0^+,1}$ transition has a reduced strength of 0.077 W.u.; this is an example of a rule discussed by Maripuu¹⁸ which states that $M1 \Delta T = 1$ transitions within a given j shell are inhibited for $j = l - \frac{1}{2}$ (and enhanced for $j = l + \frac{1}{2}$). This strength is comparable with the summed $M1 \Delta T = 1$ decay strength for the 461- and 666-keV levels which was measured to be 0.053 ± 0.004 W.u. The actual transition strengths may depend sensitively on small admixtures in the wave functions; for example, admixtures of a few percent in intensity of the $s_{1/2}^2 d_{3/2}^4$ configuration into the three states could be sufficient to reproduce the measured transition strengths.

The transition strengths from the $(2^+, 0)$ 1230-keV level may be compared qualitatively with strengths calculated for the configurations given in the preceding paragraph. The summed $M1 \Delta T = 0$ transition strength to the $(1^+, 0)$ levels of 0.004 W.u. can be compared with the calculated $[s_{1/2}^3 d_{3/2}^3]_{2^+,0} \rightarrow [s_{1/2}^3 d_{3/2}^3]_{1^+,0}$ $M1$ strength of 0.01 W.u. The measured $M1$ strength to the $(3^+, 0)$ level is much weaker, which would agree with the expectation that the $(3^+, 0)$ level is predominantly $[s_{1/2}^4 d_{3/2}^2]$, whereas this configuration must

be absent from the $(2^+, 0)$ level. Finally, the measured $(2^+, 0) \rightarrow (3^+, 0)$ $E2$ strength of 1 W.u. is comparable to the $E2$ strength of 1.1 W.u. for the $[s_{1/2}^3 d_{3/2}^3]_{2^+,0} \rightarrow [s_{1/2}^4 d_{3/2}^2]_{3^+,0}$ transition, calculated using an effective proton charge of $1.5e$, an effective neutron charge of $0.5e$, and flat radial wave functions. These comparisons are not meant to imply that the above configurations provide the only sources of transition strengths but are merely intended to provide a basis for a qualitative appreciation of the size of these strengths.

Detailed shell-model calculations^{19,20} of the $M1 \Delta T = 1$ transition strength are able to reproduce the relative decay strength in the $(1^+, 0)$ levels, but the summed strength is calculated to be about a factor of 4 greater than is measured experimentally. The inclusion of a tensor interaction in the calculations²⁰ does not reduce this discrepancy. Agreement is obtained between calculated and measured values for some of the $\Delta T = 0$ transitions, but in general appreciable differences exist, the most serious of which is the overestimate of the $M1 \Delta T = 0$ summed strength from the $(2^+, 0)$ level to the $(1^+, 0)$ levels by a factor of 50 in the calculation of Ref. 20.

¹H. D. Graber and G. I. Harris, Phys. Rev. **188**, 1685 (1969).

²F. Brandolini, I. Filosofo, C. Signorini, and M. Morando, Nucl. Phys. **A149**, 401 (1970).

³F. Brandolini, R. G. R. Engmann, and C. Signorini, Nucl. Phys. **A149**, 411 (1970).

⁴D. H. Sykes, Nucl. Phys. **A149**, 418 (1970).

⁵P. M. DeLuca, J. C. Lawson, and P. R. Chagnon, Bull. Am. Phys. Soc. **15**, 566 (1970).

⁶P. M. Endt and C. Van de Leun, Nucl. Phys. **A105**, 1 (1967).

⁷B. H. Wildenthal, G. M. Crawley, and W. McLatchie, Bull. Am. Phys. Soc. **15**, 484 (1970).

⁸J. R. Erskine, D. Crozier, J. P. Schiffer, and W. P. Alford, Bull. Am. Phys. Soc. **15**, 484 (1970); and to be published.

⁹T. K. Alexander, K. W. Allen, and D. C. Healey, Phys. Letters **20**, 402 (1965).

¹⁰K. W. Jones, A. Z. Schwarzschild, E. K. Warburton,

and D. B. Fossan, Phys. Rev. **178**, 1773 (1969).

¹¹A. Z. Schwarzschild and E. K. Warburton, Ann. Rev. Nucl. Sci. **18**, 265 (1968).

¹²J. B. Marion, Nucl. Data **A4**, 301 (1968).

¹³R. C. Greenwood, R. G. Helmer, and R. J. Gehrke, Nucl. Instr. Methods **77**, 141 (1970).

¹⁴M. L. Roush, M. A. Wilson, and W. F. Hornyak, Nucl. Instr. Methods **31**, 112 (1964).

¹⁵K. A. Snover, J. M. McDonald, D. B. Fossan, and E. K. Warburton, Bull. Am. Phys. Soc. **15**, 1665 (1970).

¹⁶D. H. Wilkinson, in *Nuclear Spectroscopy*, edited by F. Ajzenberg-Selove (Academic Press Inc., New York, 1960), Pt. B, p. 859 ff.

¹⁷G. Morpurgo, Phys. Rev. **110**, 721 (1958).

¹⁸S. Maripuu, Nucl. Phys. **A123**, 357 (1969).

¹⁹B. H. Wildenthal, to be published.

²⁰D. Evers and W. Stocker, Phys. Letters **33B**, 559 (1970).